JOURNAL OF CHEMICAL INFORMATION AND MODELING

Article

pubs.acs.org/jcim

Pharmacophore-Based Virtual Screening and Experimental Validation of Novel Inhibitors against Cyanobacterial Fructose-1,6-/Sedoheptulose-1,7-bisphosphatase

Yao Sun,[†,∥] Rui Zhang,[‡,∥] Ding Li,[§,∥] Lingling Feng,*[,†] Di Wu,[†] Lina Feng,[†] Peipei Huang,[†] Yanliang Ren,[†] JiangTao Feng,[†] San Xiao,[†] and Jian Wan*[,†]

[†]Key Laboratory of Pesticide & Chemical Biology (CCNU), Ministry of Education, and College of Chemistry, Central China Normal University, Wuhan 430079, China

[‡]College of Chemistry and Molecular Sciences, Wuhan University, Wuhan 430072, China

[§]Department of Chemistry and Chemical Engineering, College of Science, Northwest A&F University, 3 Taicheng Road, Yangling, Shanxi 712100, China

ABSTRACT: Cyanobacterial fructose-1,6-/sedoheptulose-1,7-bisphoshatase (cy-FBP/SBPase) is a potential enzymatic target for screening of novel inhibitors that can combat harmful algal blooms. In the present study, we targeted the substrate binding pocket of cy-FBP/SBPase. A series of novel hit compounds from the SPECs database were selected by using a pharmacophore-based virtual screening strategy. Most of the compounds tested exhibited moderate inhibitory activities (IC_{50} = 20.7−176.9 μM) against cy-FBP/SBPase. Compound **2** and its analogues **10** and **11** exhibited strong inhibitory activities, with IC_{50} values of 20.7, 13.4, and 19.0 μM against cy-FBP/SBPase in vitro and EC_{50} values of 12.3, 10.9, and 2.9 ppm against cyanobacteria *Synechocystis* PCC6803 in vivo, respectively. The compound **10** was selected in order to perform a refined docking study to investigate the rational binding mode of inhibitors with cy-FBP/SBPase. Furthermore, possible interactions of the residues with inhibitors were examined by site-directed mutagenesis, enzymatic assays, and fluorescence spectral analyses. The results provide insight into the binding mode between the inhibitors and the substrate binding pocket. The observed theoretical and experimental results are in concert, indicating that the modeling strategies and screening methods employed are appropriate to search for novel lead compounds having both structural diversity and high inhibitory activity against cy-FBP/SBPase.

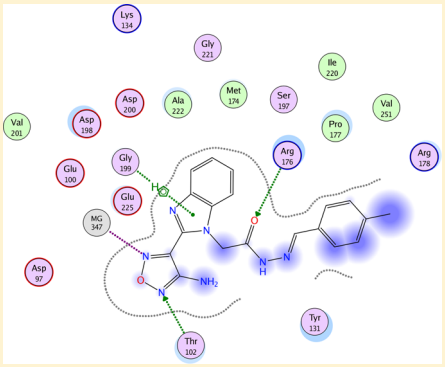

INTRODUCTION

Cyanobacteria produce harmful algal blooms (HABs), which are a growing cause of water pollution worldwide and a hazard to animal and human health.[1,2] It is of general interest to find an efficient way to reduce their harmful effects on human health, living resources, and water safety. There are several approaches for controlling HABs, including mechanical, physical, chemical, and biological controls.[3,4] Chemical control is regarded as one of the most effective methods to solve HABs. Chemical control involves the use of compounds such as copper compounds, chemical oxidants, and herbicides.[3,4] However, none of these compounds was designed or developed to target cyanobacteria specifically; thus, they are hazardous to human beings and animals. Furthermore, their utilities have significant limitations. In recent years, the method of pharmacophore-based virtual screening of novel inhibitors has become very effective in shortening the inhibitor discovery timeline.[5−7] Thus, enzymes that specifically target cyanobacteria may provide useful solutions for the development of a potential algicide.

Cyanobacteria fructose-1,6-/sedoheptulose-1,7-bisphosphatase (cy-FBP/SBPase) is a special kind of fructose-1,6-bisphosphatase (FBPase, EC 3.1.3.11) that can hydrolyze both fructose-1,6-bisphosphate (FBP) and sedoheptulose-1,7-bisphosphate (SBP).[8,9] Previous studies have shown that disruption of the cy-FBP/SBPase gene is a lethal mutation in the cyanobacteria *Synechocystis* PCC6803 and *Synechococcus* PCC7942.[10] Overexpression of cy-FBP/SBPase in transgenic tobacco leads to an increase in photosynthetic capacity in the source leaves, carbohydrate accumulation, and an accelerated growth rate.[11] These facts indicate that cy-FBP/SBPase plays a vital role in gluconeogenesis and the photosynthetic carbon reduction pathway and is actually an optimal candidate for enzymatic target searching for specific algicides to eliminate HABs. In our previous study, we determined the crystal structures of cy-FBP/SBPase complexes (PDB entries 3ROJ and 3RPL).[12] These structures reveal detailed characterizations of the active site of cy-FBP/SBPase that form a solid basis for computational screening. They enable the use of the pharmacophore-based virtual screening method to discover novel inhibitors against cy-FBP/SBPase. Furthermore, the

Received: December 19, 2013
Published: February 13, 2014

ACS Publications © 2014 American Chemical Society

dx.doi.org/10.1021/ci4007529 | *J. Chem. Inf. Model.* 2014, 54, 894−901

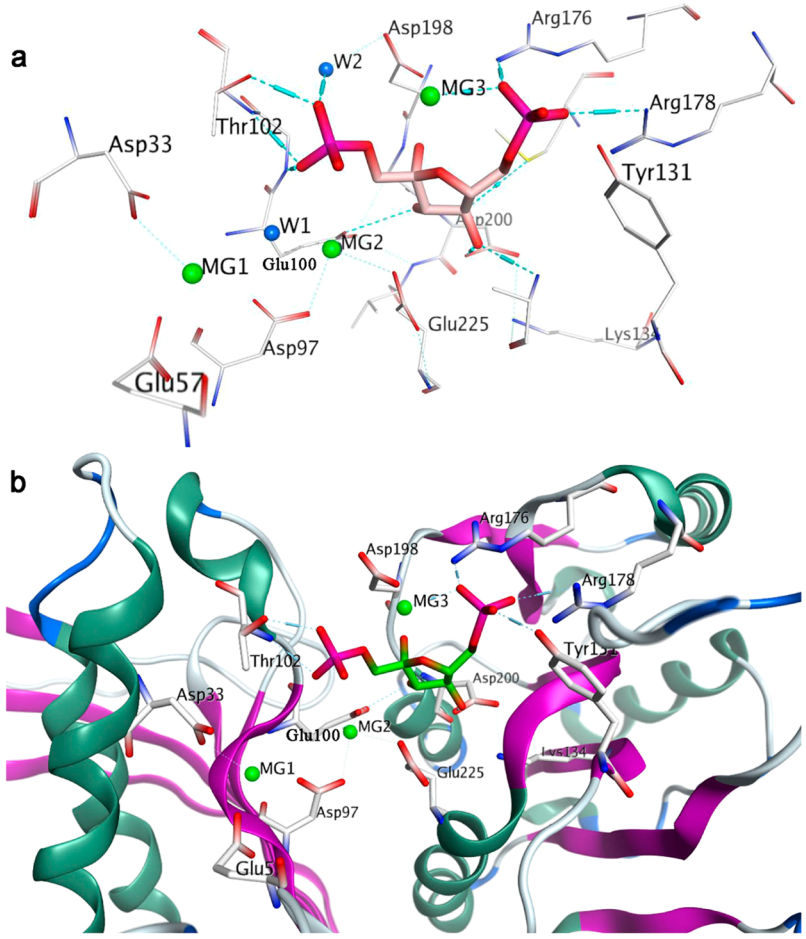

Figure 1. Structure analysis of the substrate binding pocket in cy-FBP/SBPase-AMP/+FBP. (a) The interacting molecule shown in ball-stick representation, water molecules as blue spheres and Mg^{2+} as green spheres; and the carbon atoms of protein are rendered in gray-white. The hydrogen-bonds between FBP and FBP/SBPase are shown as blue dashes. (b) Schematic diagram of the residues interacting with FBP in the substrate binding pocket of cy-FBP/SBPase. Mg^{2+} as green sphere.

reliability of this method has been well-documented in our previous studies.[13]

Although mammalian FBPase represents a highly attractive drug target for type-II diabetes, most of the previously reported or existing human FBPase inhibitors are targeted to the adenosine monophosphate (AMP) binding pocket of FBPase.[14,15] Our previous studies showed that the allosteric inhibitor AMP and the substrate FBP exhibit an unusual binding mode when they form a complex with cy-FBP/SBPase.[12] AMP is bound to the allosteric site near the interface across the up−down subunit pairs assembled in the center of the tetramer, while FBP binds opposite to the interface between the horizontal subunit pairs.[12] In the cy-FBP/SBPase complex, the substrate FBP is located in the potential active site of each monomer while the AMP domain is assembled from several residues from two different monomers.[12] The AMP binding model of cy-FBP/SBPase is different from that for the human FBPases, which makes it difficult to target the AMP domain of cy-FBP/SBPase to screen inhibitors against cy-FBP/SBPase using the pharmacophore-based virtual screening method.

In the present study, we anchored an inhibitor core in a substrate binding pocket (not in the AMP binding pocket) in an attempt to overcome the difficulty of targeting the AMP domain assembled by different monomers of cy-FBP/SBPase. Our strategy was to target the substrate binding pocket and virtually filter out a series of potential hit compounds from the SPECs database by using the pharmacophore-based virtual screening method. In vitro inhibitory assays for these compounds were carried out, and then a hit compound with a new structural scaffold and high inhibitory activity was selected to perform the refined docking study. Moreover, to validate the rational binding mode, we examined the interactions of the residues with ligands in the docking study by combining a molecular docking study with site-directed mutagenesis, enzymatic assays, and fluorescence spectral analyses.

RESULTS AND DISCUSSION

Pharmacophore-Based Virtual Screening of Inhibitors against cy-FBP/SBPase. We did a thorough analysis of the different crystal structures, particularly the substrate binding pocket, before the virtual screening of inhibitors against cy-FBP/SBPase. In our previous studies, we crystallized and determined the first crystal structures of the complexes of cy-FBP/SBPase and AMP with and without FBP (PDB entries 3ROJ and 3RPL, respectively).[12] The high-resolution crystal structures of the enzyme−ligand complexes revealed the active-site architecture and ligand binding mode as well as the network of electrostatic, hydrogen-bonding, and van der Waals interactions associated with ligand binding. Furthermore, we identified a series of residues that are important for substrate

dx.doi.org/10.1021/ci4007529 | J. Chem. Inf. Model. 2014, 54, 894−901

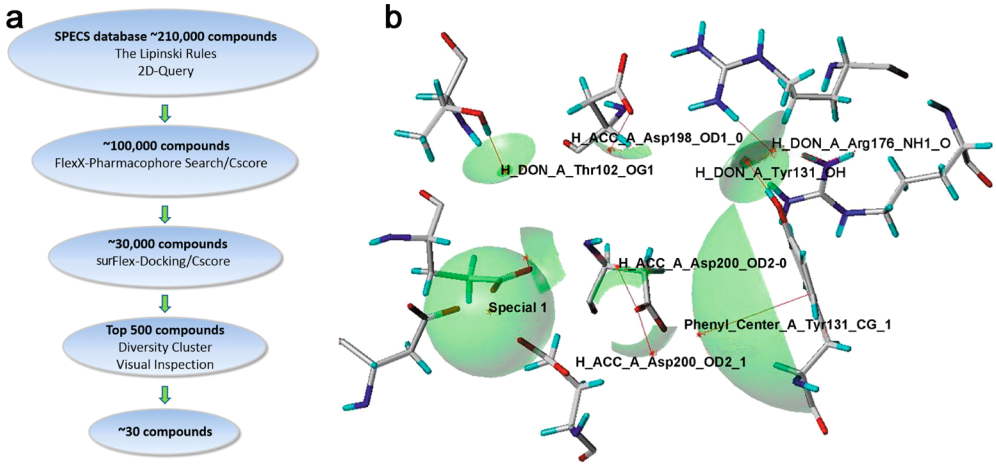

Figure 2. (a) Schematic diagram of the pharmacophore-based high-throughput virtual screening protocol. (b) Schematic diagram of pharmacophore binding mode of the active site of cy-FBP/SBPase deduced using FlexX-Pharm. Definitions: H_ACC, H-bond acceptor; H_DON, H-bond donor; Special 1, metal ion (Mg^{2+}) interaction region; Phenyl_Center, hydrophobic or conjugated $\pi-\pi$ interaction.

binding and catalytic activity and provided molecular details of the interaction between cy-FBP/SBPase and FBP by site-directed mutagenesis and kinetic experiments.[12] These studies facilitated the use of the pharmacophore-based virtual screening method for the discovery of novel inhibitors against cy-FBP/SBPase.

The substrate pocket of cy-FBP/SBPase + AMP + FBP (PDB entry 3RPL) has three metal ions (Mg^{2+}) and three water molecules, while the substrate pocket of cy-FBP/SBPase + AMP (PDB entry 3ROJ) has two metal ions (Mg^{2+}) and two water molecules. The comparison of 3RPL and 3ROJ showed that the two metal ions (MG1and MG2) and the two water molecules (W1 and W2) play an important role in stabilizing the conformation of the pocket, and they are conserved in every monomer (Figure 1a). Remarkable hydrogen bonding between FBP and its surrounding residues (T102, R176, and R178) was observed in the crystal structures (Figure 1b). Our previous studies showed that although the T102A mutant had a similar affinity ($1/K_m$) as the wild-type enzyme, its K_{cat} was reduced ($K_{cat\text{-}WT}/K_{cat\text{-}T102A}$ = 15), suggesting that T102 plays a central role in substrate (FBP or SBP) hydrolysis.[12] The substrate affinity ($1/K_m$) and K_{cat} of the R176A mutant decreased synchronously, suggesting that R176 is involved in substrate binding and hydrolysis simultaneously.[12] The R178G mutant had a similar K_{cat} as the wild-type enzyme but a lower substrate affinity [$(1/K_{m\text{-}WT})/(1/K_{m\text{-}R178G})$ = 7), suggesting that R178 is involved in substrate binding. The conserved magnesium ions (MG1 and MG2) are bound to the side chains of negatively charged residues such as D33, D97, E100, and E225 (Figure 1b). The residue mutants D33A, D97A, E100A, and E225A lost nearly all of their FBPase or SBPase activity, suggesting that these residues are important for substrate or metal binding and/or catalysis.[12] The conserved metal ions (MG1 and MG2) are important for conformational stability and are quite close to the substrate binding pocket, and they were regarded as a cationic feature when the pharmacophores were built.

The pharmacophore model (Figure 2b) was created by a thorough analysis of the substrate binding pocket of cy-FBP/SBPase. The important pharmacophore features the following constraint: H-bond donors of the side chain of T102 and R176, a spatial hydrophobic or conjugated $\pi-\pi$ interaction defined by Y131 (Phenyl_Center), and a spatial constraint defined by the distance to the metal ion (MG1 or MG2) within 3.0 Å (Special 1). Other binding active sites, namely, D200 (H-bond acceptor, hydrophilic) and D198 (negatively charged), together with the metal ion MG3 (anchored between the two phosphate anions, closer to the 6-phosphate anion) construct the active pocket, which is potentially responsible for trapping the 6-phospate anion part of the substrate FBP. According to this analysis, these residues (T102, R176, Y131, D200, and D198) and the constraint Special 1 are regarded as the important factors for the cy-FBP/SBPase inhibitor virtual screening. All of these were set as optional pharmacophore constraints. The accepted poses fulfilled at least two of these optional constraints in the cavity of cy-FBP/SBPase, and a partial match was allowed during pharmacophore-based virtual screening.

On the basis of the constructed pharmacophore model, a special protocol for virtual screening of inhibitors was generated and performed to obtain the hit compounds against cy-FBP/SBPase (Figure 2a). We filtered a set of 210 000 compounds from the SPECs database in several steps and discarded the molecules that did not meet our criteria in each step (Figure 2a). In the first step of our virtual screening strategy, we performed a 2D-ligand-based search in terms of Lipinski rules to filter the compounds from the SPECs database.[16] Thereafter, all of the selected 2D compounds (about 100 000) were transformed to 3D conformations using the CONCORD module of SYBYL 7.3 (http://www.certara.com) and then screened against our pharmacophore model using a FlexX-Pharm pharmacophore search and Cscore (Figure 2a).

FlexX-Pharm is a very popular pharmacophore-based constraint docking method that rapidly obtains the desired structures from a large database.[17−19] FlexX-Pharm docking was adopted to filter the cy-FBP/SBPase inhibitors out of the remaining 100 000 compounds to raise the efficiency of virtual screening. Following the FlexX-Pharm docking processes for cy-FBP/SBPase, a set of nonconstrained molecular docking processes (FlexX/Cscore) were performed in the same cavity to re-evaluate the receptor−ligand binding interactions and cross-validate the binding modes. This provided another set of FlexX scoring distributions for the selected compounds. Subsequently, Surflex-docking for cy-FBP/SBPase was performed on the remaining 30 000 compounds. Surflex-docking provided a significant improvement in the binding affinities of

dx.doi.org/10.1021/ci4007529 | J. Chem. Inf. Model. 2014, 54, 894−901

Scheme 1. Structures and Inhibitory Activities (IC_{50}) of Various Inhibitors against cy-FBP/SBPase in Vitro and the Corresponding Inhibitory Activities (EC_{50}) against *Synechocystis* sp. PCC6803 in Vivo

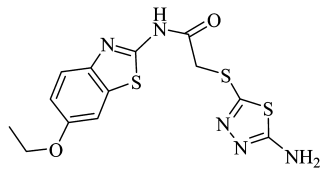

1. IC_{50} 32.4 ± 0.3 μM

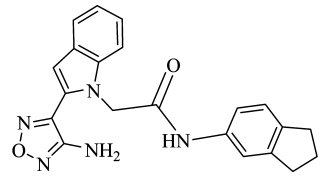

2. IC_{50} 20.7 ± 0.1μM

EC_{50} 12.3 ± 1.6 ppm

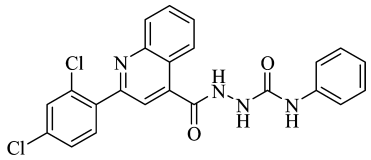

3. IC_{50} 31.3 ± 0.4 μM

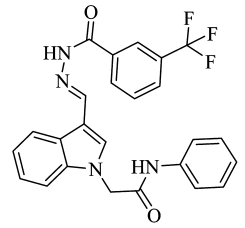

4. IC_{50} 34.2 ± 1.9 μM

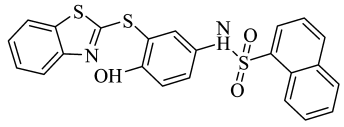

5. IC_{50} 75.7 ± 0.6 μM

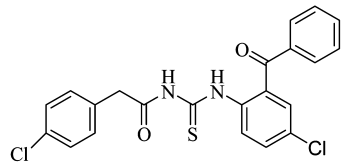

6. IC_{50} 104.8 ± 5.8 μM

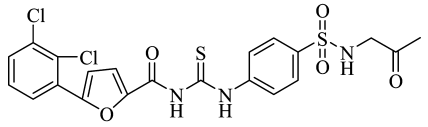

7. IC_{50} 112.4 ± 5.6 μM

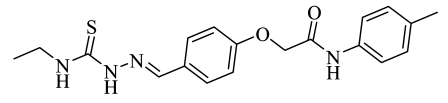

8. IC_{50} 176.9 ± 0.7 μM

the target and poses. Furthermore, it was particularly successful at eliminating false positive results while still retaining a large number of active compounds. The FlexX-Pharm and Surflex-docking procedures were also applied in our previous studies.[13] After the Surflex-docking/Cscore processes, the top 500 compounds were screened out by jointly considering dock scoring and docked conformation. The molecules that did not match the pharmacophore model well after docking were discarded. Compounds with similar backbones were categorized together, from which the "best" ones were selected jointly using Cscore, docked conformation, and the logP value for each compound. Finally, the representative 30 potential compounds were commercially bought from SPECs Corporation for biological evaluation.

Validation of the Binding Model of Hit Compounds against cy-FBP/SBPase. We evaluated the inhibitory activities of the 30 compounds acquired from the SPECs Corporation against cy-FBP/SBPase. The eight compounds shown in Scheme 1 exhibited moderate inhibitory activities against cy-FBP/SBPase (IC_{50} = 20.7−176.9 μM). Especially, compound **2** exhibited the strongest inhibitory activity among these compounds, with an IC_{50} value of 20.7 μM against cy-FBP/SBPase in vitro. Therefore, the in vivo inhibitory activity of compound **2** against cyanobacteria *Synechocystis* PCC6803 was also determined (EC_{50} = 12.3 ppm). Furthermore, by a similarity search using SPECs with a similarity of higher than 75%, we selected a series of analogues of compound **2** that were predicted to interact with the substrate catalytic active site via hydrogen-bonding, electrostatic, and other interactions (Scheme 2). By biological evaluation, most of the analogues exhibited higher inhibitory activities against cy-FBP/SBPase (IC_{50} = 13.4−39.7 μM). Especially compound **10** exhibited the highest inhibitory activity, with an IC_{50} of 13.4 μM against cy-FBP/SBPase in vitro and an EC_{50} of 10.9 ppm against cyanobacteria *Synechocystis* PCC6803 in vivo.

We further validated the binding mode of cy-FBP/SBPase with an inhibitor by using compound **10** to perform a refined docking study and site-directed mutagenesis and enzymatic assays. The potential interaction between compound **10** and the FBP binding site is shown in Figure 3. For compound **10**, the binding mode is regarded as the rational binding mode because of the higher binding affinity and the lower conformational strain. This suggests that the two different directional hydrogen bonds and the weak hydrophobic interaction help compound **10** bind in this pocket (Figure 3). Compound **10** is anchored to the substrate binding pocket and has a relatively tight interaction with T102 and R176 by hydrogen bonding. The nitrogen on the 1,2,5-oxadiazole ring is connected to the side chain of T102, which is a likely contributor to the strong binding of compound **10** (Figure 3b).

dx.doi.org/10.1021/ci4007529 | J. Chem. Inf. Model. 2014, 54, 894−901

Scheme 2. Structures and Inhibitory Activities (IC_{50}) of Compound 2 and Its Analogues against cy-FBP/SBPase in Vitro and Their Corresponding Inhibitory Activities (EC_{50}) against *Synechocystis* sp. PCC6803 in Vivo

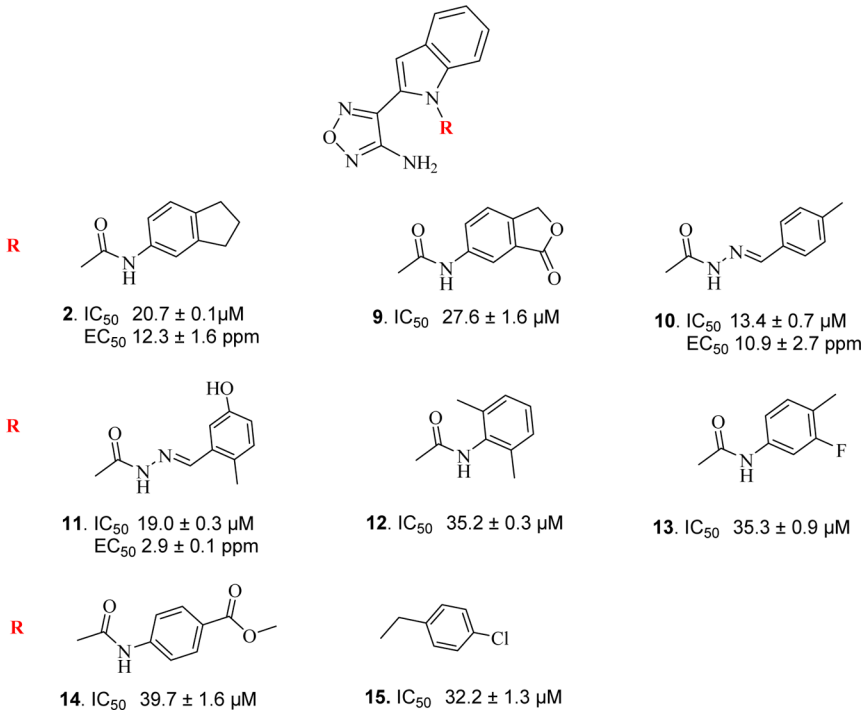

In line with our docking prediction, the IC_{50} of compound **10** against the T102A mutant (211.9 μM) was about 13-fold higher than that against the wild-type enzyme (13.3 μM) (Table 1). The experimental result revealed that the mutation of T102 to Ala can remarkably affect the inhibitory activity. Compound **10** has another hydrogen bond with R176 that is very strong and greatly improves the binding affinity. A good distance and orientation between the H-bond acceptor (compound **10**) and the H-bond donor (R176) further enhances the binding affinity. The IC_{50} of compound **10** against the R176A mutant (51.2 μM) was about 3.8-fold higher than that against the wild-type enzyme (13.3 μM) (Table 1). The negatively charged nitrogen of the 1,2,5-oxadiazole moiety has an ionic interaction with a metal (Mg^{2+}) ion. The pharmacophore feature Special 1, the spatial constraint defined by a distance to the metal ion (MG1 and MG2) within 3.0 Å, contains the metal ions and their induced coordinated binding/catalytic active points D33, D97, E100, and E225. The enzymatic activities of the D33A, D97A, E100, and E225A mutants were too low, and therefore, fluorescence spectral analyses were used to determine the binding constant (K_b) values of these residues (Table 2). The results showed that E100 and E225 are also important for the binding of compound **10** to the substrate pocket, whereas D33 and D97 have little effect on the binding of compound **10** to the enzyme cy-FBP/SBPase. These results suggest that MG2 is more important than MG1 for the binding of compound **10** to the substrate pocket. Several hydrophobic residues such as Y131, A222, M174, and P177 create a small region fit for the hydrophobic group. The crystal structure (3RPL) shows that the five-membered ring of FBP is located in this small region. A benzimidazole moiety is located in the region of the five-membered ring in compound **10** (Figure 3b). Site-directed mutagenesis and enzymatic assays showed that the IC_{50} of compound **10** against the Y131A mutant (75.6 μM) is about 5.7-fold higher than that against the wild-type enzyme (13.3 μM) (Table 1), suggesting that the small hydrophobic region is also an important pharmacophore feature. Although K134 and D200 do not have visible interactions with compound **10**, the electropositive K134 has a strong electrostatic interaction with electronegative D200 and the backbone of A222. The mutation of K134 or D200 to Ala would result in the loss of this strong electrostatic interaction and would greatly affect the conformation of the pocket and the binding of compound **10**. In line with our docking prediction, the IC_{50} values of compound **10** against the K134A mutant (114.9 μM) and D200A mutant (99.3 μM) are about 8.6-fold and 7.5-fold higher than that against the wild-type enzyme (13.3 μM), respectively (Table 1).

The inhibitory activity of compound **10** against cy-FBP/SBPase was higher than that of compound **2**. The docking results showed that the hydrophobic toluene group of compound **10** extends out of the pocket and is exposed to the solvent, which has a negative effect on the binding of compound **10**. However, the dihydroindenyl group of compound **2** (instead of a toluene group) located in this region is more hydrophobic and has a lower affinity to wild-type cy-FBP/SBPase than compound **10**. This explains the higher inhibitory activity of compound **10** against cy-FBP/SBPase compared with compound **2**. These results further validate and help in understanding the binding mode between the inhibitors and the substrate binding pocket.

CONCLUSION

In the present study, we used a pharmacophore-based virtual screening strategy to filter out a series of potential compounds with structural diversity from the SPECs database. Our strategy helped in the thorough structural analysis of the substrate binding pocket in cy-FBP/SBPase. Among these compounds, compound **2** and its analogues **10** and **11** exhibit high inhibitory activities, with IC_{50} values of 20.7, 13.4, and 19.0 μM,

dx.doi.org/10.1021/ci4007529 | J. Chem. Inf. Model. 2014, 54, 894−901

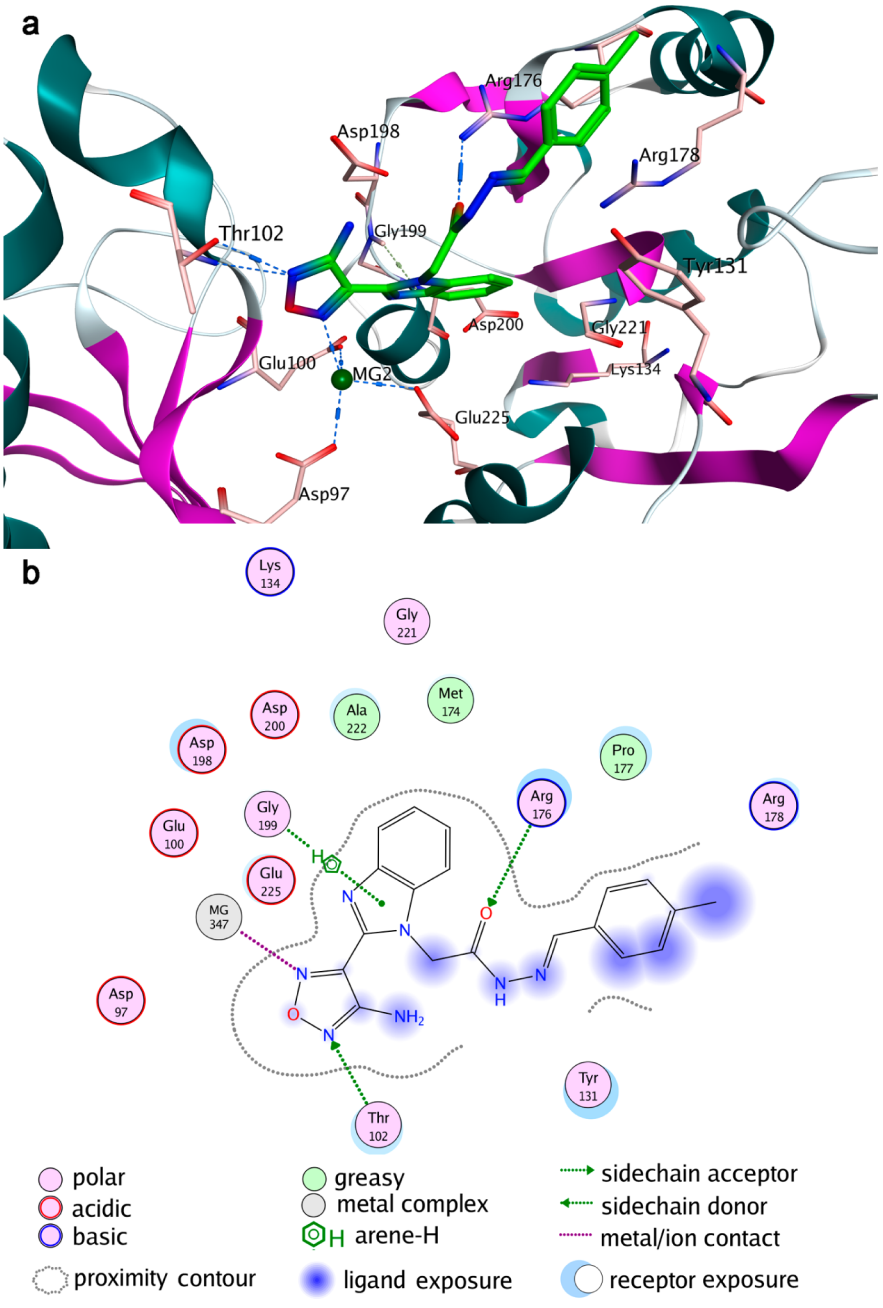

Figure 3. (a) 3D map of the potential binding mode of compound **10** targeted into the substrate binding pocket of cy-FBP/SBPase. The critical residues that could interact with compound **10** are shown. (b) 2D interaction map of interactions between compound **10** and the substrate binding pocket of cy-FBP/SBPase.

Table 1. IC_{50} Values of Hit Compound 10 against Wild-Type (WT) cy-FBP/SBPase and Various Mutants (The Substrate is FBP and the Metal Ion is Mg^{2+})

	WT	T102A	K134A	D200A	R176A	Y131A	D198H	R178G
IC_{50} (μM)	13.3 ± 0.6	179.7 ± 27.5	114.9 ± 4.1	99.3 ± 2.1	51.2 ± 2.2	75.6 ± 6.7	60.2 ± 0.72	25.6 ± 12.2
$IC_{50\text{-mutant}}/IC_{50\text{-WT}}$	1	13.5	8.6	7.5	3.8	5.7	4.5	1.9

respectively, against cy-FBP/SBPase in vitro. The EC_{50} values of compounds **2**, **10**, and **11** were 12.3, 10.9, and 2.9 ppm, respectively, against cyanobacteria *Synechocystis* PCC6803 in vivo. Compound **10** was used as the probe molecule for refined docking. The potential pharmacophore model of cy-FBP/SBPase was further investigated by combining molecular docking with site-directed mutagenesis and enzymatic assays. Our results show that several residues (T102, R176, E100, E225, D200, and K134) and the reserved metal ions (MG2) located in substrate binding pocket are essential pharmacophore features for the binding of hit compounds. The small hydrophobic region comprising Y131, A222, M174, and P177 is also an important pharmacophore feature. The combined theoretical and experimental results will facilitate the future

dx.doi.org/10.1021/ci4007529 | J. Chem. Inf. Model. 2014, 54, 894−901

Table 2. Binding Constants (K_b) for the Binding of Compound 10 to Wild-Type (WT) cy-FBP/SBPase and Various Mutants As Determined by Fluorescence Spectral Analyses

	WT	D33A	D97A	E100A	E225A
K_b (10^4 M^{-1})	2.99	6.77	3.00	0.35	1.1
$K_{b\text{-}WT}/K_{b\text{-}mutant}$	1	0.44	1	8.5	2.7

discovery of novel lead compounds with structural diversity and high inhibitory activity against cy-FBP/SBPase.

EXPERIMENTAL PROCEDURES

Pharmacophore-Based Virtual Inhibitor Screening. In order to explore the accurate binding model for the substrate binding pocket of cy-FBP/SBPase with its ligands, we carried out molecular docking analysis using the FlexX-Pharm method based on the target enzyme structure.[17−19] The virtual screening strategy principally consisted of one step of 2D ligand-based searching in terms of Lipinski rules and two steps of 3D receptor−ligand binding mode-based molecular docking by FlexX-Pharm evaluations. The Lipinski rules [≤5 H-bond donors (number of OH and NH groups), ≤10 H-bond acceptors (number of O or N atoms), MW ≤ 500 Da, MlogP ≤ 5] were employed to filter all of the molecules out of the SPECs database. FlexX is a fast automated docking method that takes the ligand's conformational flexibility into account during the docking process by an incremental fragment placing technique.[17−19] FlexX-Pharm enables pharmacophore-type constraints to be used in FlexX to guide ligand docking. Dockings were carried out using 20 initial conformations for each ligand, and the Surflex-Dock scoring function was used in the docking process.[17−20] FlexX as embodied in the SYBYL 7.0 package (http://www.certara.com) was used to explore the binding mode of the substrate in the active site and validate the molecular docking procedure for the specific cy-FBP/SBPase system. This was followed by a pharmacophore-based high-throughput virtual screening on the SPECs database (http://www.specs.net/snpage.php?snpageid=home). We defined the docking cavity for the substrate binding site as follows: all atoms located within 6.5 Å of any atom of the substrate in the crystal structure were selected, and the residue was included in the docking cavity if at least one of its atoms was picked out. The pharmacophore-based virtual screening of the SPECs database was performed using a similar docking process. Other default parameters in the FlexX-Pharm module were adopted in the virtual screening. The representative potential compounds were selected by jointly using the GOLD score, binding mode, structural diversity, and chemical and physical character for further bioaffinity testing in vitro. The compound with the highest inhibitory activity both in vitro and in vivo was submitted to molecular operating environment to perform refined docking. All of the calculations were performed in a CCNUGrid-based computational environment.

In order to explore the binding model for the binding of the compounds to the substrate binding pocket of cy-FBP/SBPase, refined docking analysis was carried out using the FlexX-Pharm docking method based on the target enzyme structure. Twenty-seven distinguished poses were generated in the final docking output file for compound **10**. The top 10 poses were selected for further analysis. The poses ranked at the first, third, fourth, fifth, seventh, and tenth shared a similar binding mode with cy-FBP/SBPase. This binding mode was regarded as the rational binding mode because of the higher binding affinity and the lower conformational strain.

Inhibitory Enzymatic Activity Evaluation and Site-Directed Mutagenesis of cy-FBP/SBPase. To evaluate the inhibitory activities of the compounds against cy-FBP/SBPase, the half-maximal inhibitory concentration (IC_{50}) values of the compounds were determined at the cy-FBP/SBPase enzyme level in vitro. The cloning, expression, purification, and activity determination of cy-FBP/SBPase were carried out as described previously.[21] FBP was purchased from Sigma. The compounds were purchased from SPECs Corporation. Enzyme activities were measured by a colorimetric assay based on the detection of inorganic phosphate hydrolyzed from FBP by wild-type cy-FBP/SBPase and various mutants.[21] For the determination of IC_{50} values, a standard reaction mixture contained 50 mM Tris-HCl (pH 8.0), 15 mM $MgCl_2$, 10 mM DTT, and 0.04 μg of purified enzyme. The hit compounds in increasing concentrations (ranging from 0 to 100 μM) were incubated for 5 min with cy-FBP/SBPase before the substrate (FBP) was added. IC_{50} values were determined by nonlinear least-squares fitting of the data using the Hill kinetic equations in the growth/sigmoidal model using Origin 7.0 software as described previously.[12] To evaluate the inhibitory activities of the compounds in vivo, half-maximal effective concentration (EC_{50}) values were determined in *Synechocystis* PCC6803 cyanobacterial cells obtained from Dr. Haibo Jiang (Central China Normal University). *Synechocystis* PCC6803 was cultured photoautotrophically in BG11 medium at 28 °C for 5 days until the logarithmic growth phase. The 1% cultured cells were then transferred to fresh medium containing different compounds. After 5 days of culturing, the optical densities at 680 nm were determined, and the inhibition rate and EC_{50} were calculated.

Site-directed mutagenesis of cy-FBP/SBPase was accomplished by the introduction of specific base changes into a double-stranded DNA plasmid. DNA encoding wild-type cy-FBP/SBPase cloned into pET28a was used as a template for mutagenesis. The standard PCR mixture contained 50−100 ng of template DNA and 100−200 ng of each mutagenizing primer. The methylated plasmid was digested with DpnI, and 4 μL of each reaction mixture was used to transform DH5α-competent cells. All of the mutations were confirmed by DNA sequencing. Verified plasmids containing the desired mutations were transformed into the *Escherichia coli* BL21 (DE3) strain. The mutant cy-FBP/SBPase proteins were purified in the same manner as wild-type cy-FBP/SBPase.

Fluorescence Spectral Analyses. Fluorescence spectral analyses were carried out as described previously.[21] All of the fluorescence measurements were carried out on a FluoroMax-P fluorescence spectrophotometer (HORIBA Jobin Yvon, France) equipped with a xenon lamp source and a 1.0 cm quartz cell. The fluorescence emission spectrum was recorded in the wavelength range of 300−500 nm upon excitation at 280 nm. The excitation and emission bandwidths were 4 nm. The fluorescence quenching experiments on cy-FBP/SBPase and its mutants (2 μM) were performed at different concentrations of compounds using a 1 cm path length fluorescence cuvette. The appropriate blank corresponding to the buffer was subtracted to correct for the fluorescence background. The binding constant (K_b) was calculated according to the equation $\ln[(F_0 - F)/F] = \ln K_b + n \ln [Q]$, where F_0 and F are the fluorescence intensities without and with the ligand, respectively, and [Q] denotes the concentration of the quencher. A plot of $\ln[(F_0 - F)/F]$ versus

dx.doi.org/10.1021/ci4007529 | J. Chem. Inf. Model. 2014, 54, 894−901

ln [Q] gave a straight line using least-squares analysis, and its intercept on the y axis was set equal to ln K_b.

AUTHOR INFORMATION

Corresponding Authors

*Tel/Fax: 86-27-67862022. E-mail: fll708@mail.ccnu.edu.cn (L.F.).

*Tel/Fax: 86-27-67862022. E-mail: jianwan@mail.ccnu.edu.cn (J.W.).

Author Contributions

‖Y.S., R.Z., and D.L. contributed equally to this study.

Notes

The authors declare no competing financial interest.

ACKNOWLEDGMENTS

This work was supported by the National Basic Research Program of China (973 Program, 2010CB126100), the National Natural Science Foundation of China (21373094, 21272089, 21172089, 21072073, 20873049, 20872044, 30900054, and 30800169), the Program for New Century Excellent Talents in University (NCET-06-0673), the Program for Changjiang Scholars and Innovative Research Team in University (IRT0953), the Program for Academic Leader in Wuhan Municipality (201150530150), the Special Fund for Basic Scientific Research of Central Colleges of the Ministry of Education (CCNU09A01010, CCNU10C01002, and CCNU10A02006), and the Research Fund for the Doctoral Program of Higher Education of China (200805581146).

ABBREVIATIONS

AMP, adenosine monophosphate; DTT, dithiothreitol; FBP, fructose-1,6-bisphosphate; F6P, fructose-6-phosphate; FBPase, fructose-1,6-bisphosphatase; FBP/SBPase, fructose-1,6-/sedoheptulose-1,7-bisphosphatase; HAB, harmful algal bloom; P_i, inorganic phosphate; SBP, sedoheptulose-1,7-bisphosphate.

REFERENCES

(1) Jousson, O.; Pawlowski, J.; Zaninetti, L.; Zechman, F. W.; Dini, F.; Di Guiseppe, G.; Woodfield, R.; Millar, A.; Meinesz, A. Invasive alga reaches California. *Nature* **2000**, *408*, 157−158.

(2) Anderson, D. M.; Cembella, A. D.; Hallegraeff, G. M. Progress in understanding harmful algal blooms: Paradigm shifts and new technologies for research, monitoring, and management. *Annu. Rev. Mar. Sci.* **2012**, *4*, 143−176.

(3) Zurawell, R. W.; Chen, H.; Burke, J. M.; Prepas, E. E. Hepatotoxic cyanobacteria: A review of the biological importance of microcystins in freshwater environments. *J. Toxicol. Environ. Health* **2005**, *8*, 1−37.

(4) Hudnell, H. K. The state of U.S. freshwater harmful algal blooms assessments, policy and legislation. *Toxicon* **2010**, *55*, 1024−1034.

(5) Andrade, C. H.; Pasqualoto, K. F. M.; Ferreira, E. I.; Hopfinger, A. J. Rational design and 3D-pharmacophore mapping of 5′-thiourea-substituted α-thymidine analogues as mycobacterial TMPK inhibitors. *J. Chem. Inf. Model* **2009**, *49*, 1070−1078.

(6) Dixit, A.; Gennady, M.; Verkhivker, G. M. Integrating ligand-based and protein-centric virtual screening of kinase inhibitors using ensembles of multiple protein kinase genes and conformations. *J. Chem. Inf. Model* **2012**, *52*, 2501−2515.

(7) Markt, P.; McGoohan, C.; Walker, B.; Kirchmair, J.; Feldmann, C.; Martino, G. D.; Spitzer, G.; Distinto, S.; Schuster, D.; Wolber, G.; Laggner, C.; Langer, T. Discovery of novel cathepsin S inhibitors by pharmacophore-based virtual high-throughput screening. *J. Chem. Inf. Model* **2008**, *48*, 1693−1705.

(8) Tamoi, M.; Murakami, A.; Takeda, T.; Shigeoka, S. Acquisition of a new type of fructose-1,6-bisphosphatase with resistance to hydrogen peroxide in cyanobacteria: Molecular characterization of the enzyme from *Synechocystis* PCC6803. *Biochem. Biophys. Acta* **1998**, *1383*, 232−244.

(9) Tamoi, M.; Ishikawa, T.; Takeda, T.; Shigeoka, S. Molecular characterization and resistance to hydrogen peroxide of two fructose-1,6-bisphosphatases from *Synechococcus* PCC7942. *Arch. Biochem. Biophys.* **1996**, *334*, 27−36.

(10) Tamoi, M.; Takeda, T.; Shigeoka, S. Functional analysis of fructose-1,6-bisphosphatase isozymes (ifbp-I and fbp-II gene products) in cyanobacteria. *Plant Cell Physiol.* **1999**, *40*, 257−261.

(11) Miyagawa, Y.; Tamoi, M.; Shigeoka, S. Overexpression of a cyanobacterial fructose-1,6-/sedoheptulose-1,7-bisphosphatase in tobacco enhances photosynthesis and growth. *Nat. Biotechnol.* **2001**, *19*, 965−969.

(12) Feng, L. L.; Sun, Y.; Deng, H.; Li, D.; Wan, J.; Wang, X. F.; Wang, W. W.; Liao, X.; Ren, Y. L.; Hu, X. P. Structural and biochemical characterization of fructose-1,6-/sedoheptulose-1,7-bisphosphatase from the cyanobacterium *Synechocystis* strain 6803. *FEBS J.* **2014**, *281*, 916−926.

(13) Zhang, Q. Y.; Li, D.; Wei, P.; Zhang, J.; Wan, J.; Ren, Y. L.; Chen, Z. G.; Liu, D. L.; Yu, Z. N.; Feng, L. L. Structure-based rational screening of novel hit compounds with structural diversity for cytochrome P450 sterol 14a-demethylase from *Penicillium digitatum*. *J. Chem. Inf. Model* **2010**, *50*, 317−325.

(14) Wright, S. W.; Carlo, A. A.; Carty, M. D.; Danley, D. E.; Hageman, D. L.; Karam, G. A.; Levy, C. B.; Mansour, M. N.; Mathiowetz, A. M.; McClure, L. D.; Nestor, N. B.; McPherson, R. K.; Pandit, J.; Pustilnik, L. R.; Schulte, G. K.; Soeller, W. C.; Treadway, J. L.; Wang, I. K.; Bauer, P. H. Anilinoquinazoline inhibitors of fructose-1,6-bisphosphatase bind at a novel allosteric site: Synthesis, in vitro characterization, and X-ray crystallography. *J. Med. Chem.* **2002**, *45*, 3865−3877.

(15) Erion, M. D.; Dang, Q.; Reddy, M. R.; Kasibhatla, S. R.; Huang, J.; Lipscomb, W. N.; van Poelje, P. D. Structure-guided design of AMP mimics that inhibit fructose-1,6-bisphosphatase with high affinity and specificity. *J. Am. Chem. Soc.* **2007**, *129*, 15480−15490.

(16) Lipinski, C. A.; Lombardo, F.; Dominy, B. W.; Feeney, P. J. Experimental and computational approaches to estimate solubility and permeability in drug discovery and development settings. *Adv. Drug Delivery Rev.* **1997**, *23*, 3−25.

(17) Gumede, N. J.; Singh, P.; Sabela, M. I.; Bisetty, K.; Escuder-Gilabert, L.; Medina-Hernández, M. J.; Sagrado, S. Experimental-like affinity constants and enantioselectivity estimates from flexible docking. *J. Chem. Inf. Model* **2012**, *52*, 2754−2759.

(18) Ding, F.; Yin, S.; Dokholyan, N. V. Rapid flexible docking using a stochastic rotamer library of ligands. *J. Chem. Inf. Model* **2010**, *50*, 1623−1632.

(19) Pierce, B. G.; Weng, Z. A flexible docking approach for prediction of T cell receptor-peptide−MHC complexes. *Protein Sci.* **2013**, *22*, 35−46.

(20) Fukuzawa, K.; Kitaura, K.; Nakata, K.; Kaminuma, T.; Nakano, T. Workshop 1.5 Fragment molecular orbital study of the binding energy of ligands to the estrogen receptor. *Pure Appl. Chem.* **2003**, *75*, 2405−2410.

(21) Sun, Y.; Liao, X.; Li, D.; Feng, L. L.; Li, J.; Wang, X. F.; Jin, J.; Yi, F.; Zhou, L.; Wan, J. Study on the interaction between cyanobacteria FBP/SBPase and metal ions. *Spectrochim. Acta. Part A* **2012**, *89*, 337−344.